Theor Chim Acta (1988) 73: 155–171

Theoretica Chimica Acta

An *ab initio* study of the molecular structure and vibration–rotation spectrum of the triplet radical HCCN*

Per-Åke Malmquist[1], Roland Lindh[1], Björn O. Roos[1], and Stephen Ross[2]

[1] Department of Theoretical Chemistry, Chemical Centre, University of Lund, P.O.B. 124, S-221 00 Lund, Sweden

[2] Department of Chemistry, University of Alberta, Edmonton, Alberta, Canada T6G 2G2

The bent triplet cyanocarbene H-C-C≡N and the linear triplet allene H-C=C=N have been studied by the CASSCF and CI methods, using a DZP basis. Relaxation of all geometrical parameters for the CASSCF energy results in a bent molecule with CCH angle 133° and a barrier to linearity of 6.4 kcal/mol, which was lowered to 2.3 kcal/mol in a subsequent CI calculation. The Davidson correction lowered it further to 1.8 kcal/mol.

A 26-term analytical potential energy surface (PES) was fitted to CASSCF, CI, and Davidson corrected CI energies in 94 different geometries. Using these three potentials, the semi-rigid bender model predicts a CCH bending frequency of 782, 505, and 503 cm^{-1}, resp., which compares favourably with an experimentally observed IR transition line at 458 cm^{-1}. For the deuterated species, the corresponding frequencies are 610, 407, and 402 cm^{-1}, to be compared with two possible absorption lines at 405 and 317.5 cm^{-1}.

The PES was then parametrized by adding a variable CCH angle dependence, and a comprehensive vibration-rotation spectrum was calculated variationally, using the exact 4-atom vibration-rotation kinetic Hamiltonian, for a range of barrier heights. Comparison with experiment indicates a barrier in the range 1 ± 0.5 kcal/mol.

Key words: HCCN — Vibration-rotation — Potential energy surface

1. Introduction

The first spectroscopic studies of HCCN was reported by Bernstein et al. [1]. The radical was produced by photolysis of a precursor in matrix isolation, and

* Dedicated to Professor J. Koutecký on the occasion of his 65th birthday

on the basis of Electron Spin Resonance (ESR) spectra, it was declared a linear triplet radical. This conclusion was confirmed by Wasserman et al. [2], who repeated the experiment in a number of matrices at 4 K. Dendramis and Leroi [3] pointed out that the apparent linearity, concluded from ESR zero-field splitting, may be an artefact of the matrix isolation. They analyzed instead infrared absorption spectra from several isotopic isomers of HCCN produced in an Ar matrix. Unpublished *ab initio* calculations had suggested two possible structures, the linear allene HC=C=N and the bent cyanocarbene HC-C≡N. They attempted to fit harmonic valence force field models based on these assumed structures to their IR frequencies, and found that the linear allene structure was probably correct. A microwave spectrum of the free radical has been obtained by Saito et al. [4], and it was concluded that the molecule is linear. Thus, all available experimental data seem to support the linear allene structure.

Ab initio calculations by Harris et al. [5], Zandler et al. [6], Kim et al. [7] and Rice and Schaefer [8], are also quite conclusive about the structure. They all find the bent carbene to be the preferred structure. They also show, however, that with increasing level of theory the barrier to linearity decreases. Kim et al. [7] calculated vibration frequencies by the harmonic oscillator approximation for the two structures. They both gave poor agreement with experiment.

There are several possible sources to the discrepancy between theory and experiment. First of all, the IR and ESR studies require matrix isolation studies, and the interaction energy with the surrounding dielectric medium may be different for the different structures. For comparison with such empirical data, theoretical studies should ideally be performed with the medium present to account for the matrix effects. Methods for such calculations are under way [9], but are not yet available.

There is no such difficulty with the microwave spectrum of the free radical. The conclusion by Saito et al. [4], that the molecule is linear, was based on the absence of satellite lines in the spectrum. However, such satellite lines will be present also for the linear molecule, and their failure to observe them is therefore due to a low signal to noise ratio. The satellite lines result from thermal excitation of low-lying states, which for the linear molecule would be described as a bending vibration and for the non-linear would go over continuously into the 1_{11} and near-lying rotational states. The low S/N ratio signifies that the excitation energy is fairly high. This, however, is not conclusive: with our model potential, a vanishing barrier gives about 230 cm^{-1}, while an 0.5 kcal/mol barrier gives about 160 cm^{-1}.

Finally, even for the free radical, ab initio quantum-mechanical calculations are not reliable enough to discriminate between different structures, when the predicted energy difference is only around one kcal/mol. It seems implausible that the precision is going to drastically improve in the near future.

Nevertheless, we feel that even with data and theoretical methods available today, much remains to be done. First, theoretically predicted vibrations have been based on the harmonic approximation, which is almost worthless in this and

similar cases. We must go beyond this approximation. Second, if the PES is parametrized, the sensitivity of any feature of the vibration spectrum to changes in the PES is not a drawback but an advantage. The effect of reasonable errors in the computed PES, as well as the effect of different surrounding dielectrics, is essentially to displace the equilibrium structure along a fairly well-defined minimum-energy path from a linear to a bent structure. Such a perturbation is easily incorporated in the theoretical PES and results in a one-parameter adjustable model. Thus, it is possible to make a systematic study of how the spectrum depends on such perturbations. Third, the already mentioned low-lying vibration-rotation states are very sensitive to molecular structure. It is desirable to know their energy as a function of the adiabatic potential. The goals of the present study are: to calculate a theoretical potential surface; to calculate accurate vibration-rotation eigenstates for this potential, with various perturbations included; to establish for future use a reasonably reliable guide to connect experimental vibration-rotation spectra with a corresponding adiabatic potential; and, if possible, to determine the molecular structure by comparison to available empirical data. All of these goals have not been reached. Nevertheless, we believe that the present results will prove useful in future studies, experimental as well as theoretical.

2. The potential surface: methods

The adiabatic potential surface was studied at three levels of approximation, namely by the Complete Active Space SCF (CASSCF) method [10], the Contracted CI (CCI) method [11], and, finally, by correcting the CCI calculation by the so-called Davidson correction [12]. For the last case, we will use the abbreviation CCI + Dav.

The CASSCF method is a form of the multi-configurational SCF method, which means that the energy is optimized with respect to variation of the orbitals as well as of the CI coefficients. The distinctive feature of CASSCF is that instead of selecting a few important configurations, every Configuration State Function (CSF) with a given spin and a specified restriction on orbital occupancy is included. The restriction is that a certain set of orbitals, the inactive orbitals, are always doubly occupied, and the remaining electrons are distributed among another set, the active orbitals, in every way compatible with desired total spin and symmetry. With a properly chosen active orbital set, all the larger variations in natural occupancy, which may occur e.g. because of bond formation or breaking, are accounted for, giving the necessary balanced treatment of different regions of the PES. The limitation of the CASSCF scheme is the very rapid growth of the CI expansion length with the size of the active space. With present techniques, this limits the number of active orbitals to around 12–14, except in very favourable special cases, and thus a large fraction of the dynamic correlation energy is left out. This part is sensitive to the electronic structure, and in particular to the amount of ionicity in the valence-bond meaning of the term. Large differences in electronic structure between different parts of the PES can therefore decrease the reliability of the CASSCF method.

To account for the changes in dynamic correlation, we make a CI calculation involving all possible single and double excitations. However, in order to treat the whole PES in a balanced way we must use a multireference CI, with a reference space comprising every CSF which has a sizeable CI coefficient in any calculation. Optimized CASSCF orbitals are used, and the reference space is selected by the size of the CI coefficients obtained in the CASSCF calculations. With a decent choice of reference space, it turns out that the multireference singles and doubles CI described here is too large to be practical, when a large number of calculations are required. Fortunately, most of the CSFs can be treated as a perturbation contribution to a much smaller set of "internal" CSF's with small loss of correlation energy [11], resulting in the Contracted CI (CCI) method.

Finally, the CCI results can be further improved by adding the Davidson correction [12]. This is intended to correct for the higher excitations missing from a singles and doubles single-reference CI, but it has been found useful also in the multi-reference case.

In all calculations, the molecule was confined to a planar structure (C_s point group), except that a linear structure (for which we used the C_{2v} point group) was assumed in some exploratory calculations. The ground electronic state in all calculations was then $1^3A''$ (or 1^3A_2).

As atomic basis functions, we used Huzinaga's [12] H(4*s*/2*s*) and Dunning's [14] C,N(9*s*5*p*/4*s*2*p*) split-valence contracted gaussian basis sets. To these, we added standard polarization functions with exponent coefficients $\alpha_d(\mathrm{N}) = 0.75$ and $\alpha_d(\mathrm{C}) = 0.80$, and $\alpha_p(H) = 1.0$. The complete basis set includes 53 contracted gaussian functions, and is of comparable quality to those used by Zandler et al. [6] and by Kim et al. [7]. Integrals were calculated by Almlöf's MOLECULE program [15], and integral derivatives by a program written by Almlöf and Saebö [16].

In the CASSCF calculations, the active space was chosen with the aim of obtaining a balanced description of the two molecular structures and to include the most significant electronic configurations. The natural choice is to include the valence π orbitals, i.e., 3 orbitals each in irreducible representation a' and a'', which results in 99 CSFs of $^3A''$ symmetry. These calculations were made by a combined super-CI/two-step Newton-Raphson CASSCF program [10]. Initially, the stationary points of the CASSCF energy was found by automatic relaxation of analytic gradients by a program written by Saebö and Taylor [16]. The analytic gradients of the CASSCF energy with respect to the nuclear coordinates were computed as described by Taylor [17]. These programs were run on a UNIVAC/1108 computer.

In the CCI calculations, five reference CSFs were used. They were $[(8a')^2\ (9a')\ (1a'')^2\ (2a'')]$, $[(8a')\ (9a')\ (10a')\ (1a'')^2\ (2a'')]$, $[(8a')^2\ (9a')\ (1a'')\ (2a'')\ (3a'')]$, $[(8a')^2\ (9a')\ (2a'')\ (3a'')^2]$, and $[(9a')\ (10a')^2\ (1a'')^2\ (2a'')]$, above the common $[(1a')^2 \ldots (7a')^2]$ part. The core orbitals were frozen, and the three orbitals with highest orbital energy removed. With 14 electrons correlated, the number of singly or doubly excited configurations were 190 873 and 378 100 for the linear and bent

structures, resp., resulting in 3871 and 4540 contracted functions. All the CCI calculations were made on a CRAY-1S computer.

3. The potential surface: results

Starting with the structures obtained by Zandler et al. [6], the gradients were relaxed to about 0.0017 a.u. by an approximate Newton-Raphson procedure, where the new gradient in each step was used to improve the assumed force constant matrix. The update method worked best if the initial force constant matrix was deliberately underestimated. Even if the first steps are poor, final convergence rate is much improved. If the force constants are overestimated, the stationary point is essentially approached from one direction only, which gives a bad sampling of the potential surface.

In order to see if there was a second minimum with carbenic electron structure the following test was performed. The bent molecule was straightened out to almost linearity with preserved bond lengths and MO coefficients, and then allowed to relax. The molecule at once adopted an allenic electron structure and then gradually relaxed back to the bent carbene structure. This shows that the two structures are on the same PES with the bent structure as a minimum and the linear as a saddle point. Structural parameters are summarized in Table 1.

At the stationary points of the CASSCF PES, subsequent CCI calculations were made. The stability of the bent form then decreased from 6.4 kcal/mol to 2.3 kcal/mol. Adding the Davidson correction decreases the stability slightly more, to 2.2 kcal/mol. Of course, this is not precisely equal to the *barriers* since the energies were computed at the stationary points of the CASSCF energy, but the differences to the true barriers are very small. A recent calculation by Rice and Schaefer [8] gives similar results with a DZP basis. They also used a TPZ basis set in the CASSCF calculation, which shortened the bonds by about 0.01 Å. Furthermore, they used a larger reference space (16 functions) in the CCI calculation, which lowered the stability of the bent form to 0.8 kcal/mol.

Finally, we calculated CASSCF, CCI, and CCI+Dav energies at 94 different geometries around the minimum-energy path for different CCH angles from 180° to 110°. Analytic potential functions were fitted to these data, and used in the subsequent vibration-rotation analysis. Since the CH bond distance didn't change much and the CCN tail remained fairly linear in the relaxation study, they were now held fixed at 1.0725 Å and 180°, respectively. This simplification was made in order to keep the number of CCI calculations down. Structural parameters for these models has been included in Table 1. The potential energy minimum path as function of the CCH angle, as calculated from CCI+Dav energies, is described in Table 2, and the potential energy function is shown in Fig. 1.

The results may be summarized as follows: The relevant part of the PES is a long and narrow valley from a minimum with CCH angle in the 130°-140° range to a saddle point at CCH = 180°. At the minimum, the CC distance is 1.36 Å and the CN distance 1.20 Å; at the saddle point, $R_{CC} = 1.32$ Å and $R_{CN} = 1.22$ Å.

Table 1. Compilation of stationary structures obtained by different methods. Values in parentheses have been assumed

	Method	R_e(CC) (Å)	R_e(*CN*) (Å)	R_e(CH) (Å)	θ_e(CCH) (deg)	θ_e(CCN) (deg)	ΔE (kcal/mol)
Linear	RHF[a]	1.367	1.147	1.057	(180)	(180)	10.9
	CI[b]	1.353	1.208	1.080	(180)	(180)	4.3
	CISD[a]	1.340	1.184	1.064	(180)	(180)	5.1
	CISD[a]+Dav[a]	1.327	1.204	1.068	(180)	(180)	3.2
	CASSCF[c]	1.311	1.204	1.059	(180)	(180)	6.2
	CASSCF[d]	1.300	1.190	1.052	(180)	(180)	5.7
	CASSCF[e]	1.310	1.205	1.066	(180)	(180)	6.4
	CASSCF[e]	1.310	1.204	(1.073)	(180)	(180)	6.1
	CCI[e]	1.305	1.222	(1.073)	(180)	(180)	2.3
	CCI[e]+Dav[e]	1.316	1.225	(1.073)	(180)	(180)	2.1
Bent	RHF[a]	1.414	1.142	1.071	129.4	178.3	—
	CI[b]	1.400	1.194	1.085	135.3	176.8	—
	CISD[a]	1.390	1.174	1.075	134.0	176.8	—
	CISD[a]+Dav[c]	1.337	1.189	1.078	136.6	175.9	—
	CASSCF[c]	1.378	1.180	1.071	133.1	174.0	—
	CASSCF[d]	1.365	1.167	1.065	133.9	174.3	—
	CASSCF[e]	1.379	1.180	1.079	133.2	173.1	—
	CASSCF[e]	1.379	1.179	(1.073)	132.6	(180)	—
	CCI[e]	1.358	1.197	(1.073)	137.9	(180)	—
	CCI[e]+Dav[e]	1.363	1.205	(1.073)	138.3	(180)	—

[a] From [7]
[b] From [6]
[c] From [8], using double-zeta+polarization basis
[d] Same, using triple-zeta+polarization basis
[e] Our work

Table 2. Structural parameters along the CCH bending minimum-energy path, for the CCI+Dav potential energy surface ($\theta_{CCN}=180°$, $R_{CH}=1.0725$ Å)

θ_{CCH} (deg)	R_{CC} (Å)	R_{CN} (Å)	ΔE (cm^{-1})
180	1.3165	1.2247	775.6
170	1.3205	1.2225	700.6
160	1.3315	1.2173	485.7
150	1.3461	1.2111	197.3
140	1.3611	1.2057	5.5
130	1.3742	1.2019	164.8
120	1.3856	1.1994	943.3
110	1.3973	1.1979	2555
100	1.4130	1.1965	5116

Stationary points:

θ_{CCH}	$x=R_{CC}$	$y=R_{CN}$	ΔE	$k_{\theta\theta}$	$k_{\theta x}$	$k_{\theta y}$	k_{xx}	k_{xy}	k_{yy}
180.0	1.3165	1.2247	775.6	−0.0225	0.0	0.0	0.5000	0.2021	0.7096
138.33	1.3634	1.2050	0.0	0.0690	−0.0569	0.0214	0.4205	0.1320	0.8688

[a] Note: $k_{\theta\theta}$, etc, are the harmonic force constants at the stationary points, using atomic units and radians

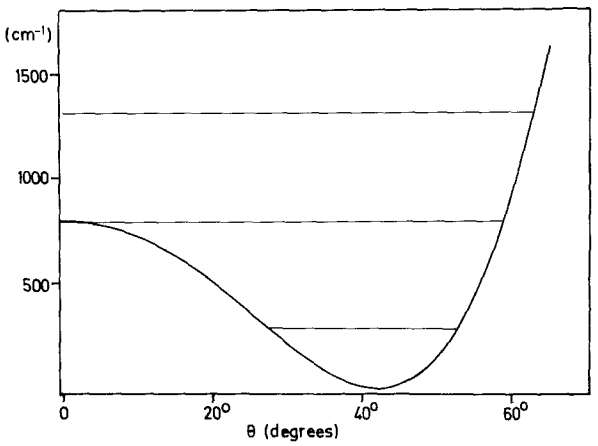

Fig. 1. The CCI potential function, and lowest vibration states in the semi-rigid bender approximation

From the relaxation study, we know that the CCN angle bends slightly in the *trans* direction when CCH is bent, and the CH bond length is slightly stretched.

The precise CCH equilibrium angle depends of course on the approximation level, but it is noteworthy that there appears to be a fairly reliable relationship between this angle and the barrier height for all calculations cited in Table 1. This is precisely what we should expect from our working hypothesis, that the difference between any two calculated surfaces, or between a calculated surface and an accurate adiabatic PED, or indeed even the change in PES induced by a surrounding dielectric medium, are all slowly varying functions of the nuclear coordinates and that only the CCH angle dependence of these differences has large observational consequences. In practical terms, we propose that by adding a term $p \cdot \cos(\theta)$ to our CCI+Dav potential surface, where θ is the complement to the CCH angle, we obtain a one-parameter adjustable PES which should be accurate enough to allow comparison with vibration-rotation spectroscopic data. The remaining errors only affect the stiffer internal coordinates, with acceptable structural consequences. The relation between parameter p and some structural data may be seen in Figs. 3 and 4 (barrier height) and in Fig. 7 (equilibrium geometry) later in the text. This potential function model was used in the subsequent vibration-rotation analysis using the full kinetic Hamiltonian. In the semi-rigid bender calculations, the actual CASSCF, CCI and CCI+Dav potential functions were used.

4. The vibration-rotation analysis

The usual approach to the vibration-rotation problem is to attempt a separation of the Hamiltonian by variable separation, into a center-of-mass kinetic term, an internal vibration term, and a rotation term. The first separation is trivial. The separation of the last two terms cannot be done exactly, except for diatomics, so an additional kinetic interaction between vibration and rotation will remain.

The use of Eckart coordinates for a suitable reference structure will often make this term small enough to be treated as a perturbation.

This approach fails in the present case. A linear reference structure cannot be used to define an Eckart frame. Even if we accept a fairly stable bent equilibrium structure, we cannot use the Eckart coordinate system since the wave function can be quite large for the linear structure, where the mapping between nuclear position and Eckart coordinates is singular. In fact, regardless of coordinate system, it is impossible to treat vibration-rotation interaction by perturbation expansion unless the wave function is negligibly small for near-linear structures. We must therefore treat the vibration-rotation interaction accurately, and a near-separability of the Hamiltonian is no longer a criterion on the suitability of the coordinate system.

Our main requirements on a model Hamiltonian for the vibration-rotation problem is that it is equally valid for all CCH angles, and that the nonlinear interdependence between CCH angle and CC and CN bond lengths is taken into account. The only simple way of doing this is to use a generalized coordinate for the CCH bending, with accompanying changes in CC and CN bond lengths predetermined from a minimum-energy path, and to hope that Hamiltonian terms involving all other internal coordinates will give an approximately constant contribution which can be dismissed. The lowest acceptable approximation is then the semi-rigid bender model of Bunker et al. [18], based on the treatment of the vibration-rotation Hamiltonian by Hougen et al. [19].

We applied the semi-rigid bender model to our unperturbed potential energy surfaces, at all three levels of approximation, and the results of some sample calculations are summarized in Table 3. The only values that can be

Table 3. Selected results from the semi-rigid bender calculation

		Ref [7][a]	CASSCF[b]	CCI[b]	CCI+Dav[b]	Exp
Barrier (cm^{-1})		3810	2 127	794	776	—
(kcal/mol)		10.9	6.1	2.3	2.1	—
ν_4 (cm^{-1})	HCCN	793	782	505	503	458[c]
	DCCN	656	610	407	402	405[c]
$E_{K=1}-E_{K=0}$	HCCN	—	—	56	—	—
(cm^{-1})	DCCN	—	—	—	—	—
$B_{v=0}$ (MHz)[d]	HCCN	—	10 862	10 791	10 703	10 986[e]
	DCCN	—	9 908	9 805	9 727	—
$q_{v=0}$(MHz)[f]	HCCN	—	134	109	106	—
	DCCN	—	196	155	150	—

[a] SDCI+Dav results from Table IV of [7] for bent HCCN, in the harmonic oscillator approximation, included for comparison

[b] Our work, using unperturbed potential energy functions

[c] Experimental values from [3]

[d] B estimated at $(E(1_{01})-E(0_{00}))/2$

[e] Experimental value from [4]

[f] q estimated as $E(1_{10})-E(1_{11})$

compared with presently available experimental data are the ν_4 vibration excitation energies and the rotation constant B. The former are much too high for the CASSCF surface, but the CCI and CCI+Dav results are in good agreement with experiment if we assign the 405 cm^{-1} line for DCCN to the ν_4 vibration. These results are encouraging but not conclusive. The CCI potential function and the lowest ν_4 excited states are shown in Fig. 1. The rotation constant B is too low. This is because our basis set has made the bond lengths about 0.01 Å too long, as noted previously.

The semi-rigid bender seems to be a reasonable approximative model, but it takes account only of the single "soft" internal coordinate for CCH bending. It does not give excitation frequencies for the other vibration modes, nor does it take any account of the interaction between the ν_4 mode and the ν_5 and ν_6 (CCN tail-wagging) modes, or between the ν_5 and ν_6 modes and the rotation of the molecule. A calculation of the lowest vibration-rotation levels using the full kinetic Hamiltonian with no approximations is somewhat complicated, but we did not want to resort to approximations with unknown errors unless it became necessary. Preliminary estimates convinced us that a variational calculation using a basis set expansion of a few tens of thousand terms would be reasonably accurate, and that such a calculation could be efficiently done on our FPS-164 computer. We found out later that the difficulties had been overestimated, and that expansion lengths of a few hundred up to a few thousand terms was enough. The first problem was to find a suitable form of the Hamiltonian. We decided in favour of a fairly simple coordinate system, see Fig. 2. A set of internal cartesian coordinates are defined by requiring that

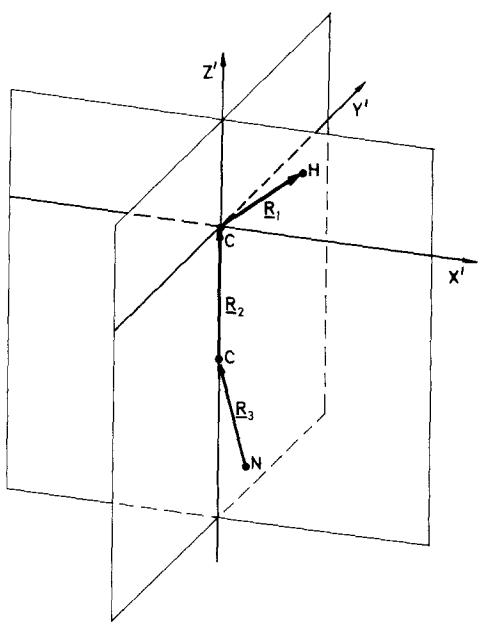

Fig. 2. Internal coordinate system used for the full kinetic Hamiltonian

$$\boldsymbol{R}_1 = a\boldsymbol{e}'_x + b\boldsymbol{e}'_z$$

$$\boldsymbol{R}_2 = c\boldsymbol{e}'_z$$

$$\boldsymbol{R}_3 = d\boldsymbol{e}'_x + e\boldsymbol{e}'_y + f\boldsymbol{e}'_z$$

where $a \geq 0$ and $c \geq 0$. Thereby, also the Euler angles for the orientation of the internal coordinate system are implicitly defined. However, the stiffness of the CH bond and the wide range of CCH angles makes it expedient to make a further coordinate transformation:

$$\boldsymbol{R}_1 = r(\sin\theta\boldsymbol{e}'_x + \cos\theta\boldsymbol{e}'_z)$$

where $r \geq 0$ and $0 \leq \theta < \pi$. This coordinate system is independent of the nuclear masses, which is an advantage since our analytic PES will be the same regardless of isotopic substitution. The kinetic Hamiltonian has about 40 more or less complicated terms, and none of these can be *a priori* neglected. This does not matter to us, of course, since we use the full Hamiltonian. The wave function is expanded in terms which are products of more primitive functions, most of which depend on only one or two internal coordinates. Each basis function contains a rotation function factor $D_{JMK}(\alpha, \beta, \gamma)$ of the Euler angles, where $M = J =$ total angular momentum, while K takes values in the range $-J, \ldots, J$.

As described earlier, the CH distance and CCN angle had been kept constant when calculating the potential energy surfaces. It is desirable to do some further electronic structure calculations at more general geometries, but we have not yet done so. One reason for waiting is that we would prefer to be able to get a dipole moment surface also, and this possibility has yet to be implemented in the CCI program. We assume that at this point, the data at hand are enough for a preliminary investigation if we supplement the PES with a simple Morse function for the CH stretch, and an isotropic two-dimensional harmonic oscillator for the excursions of the N nucleus away from the CC axis. Coupling terms to other variables were ignored.

At this stage, the results are a number of energy levels, wave functions, and expectation values of structural parameters tabulated as functions of the perturbation parameter p. At a later stage, transition probabilities may also be included. We believe that it is easiest to understand the results if all parameters of the calculation except p are held fixed. Therefore, we did not want to adjust e.g. the assumed CCN bending force constant to reproduce the experimental DCCN ν_5 transitions energy for each different value of p. After assigning to it a value which was roughly consistent with the experimental energy, it was held constant throughout the calculations.

A survey was first made of all vibrationally excited states with $J = 0$, in the energy range up to and including the CH stretching frequency ν_1. In these calculations, the CCN bending modes were "frozen" by using a single (optimized) basis function factor for the dependence on coordinates d and e. The reason for freezing the CCN bending modes was to keep the number of eigenstates in this large energy interval down. The consequences are that the ν_5 and ν_6 modes, and all

their overtones and combinations with other modes, are missing, and also that the ν_4 vibration energies are somewhat perturbed.

The excitation energies from the ground state as a function of the perturbation parameter p are shown in Figs. 3 and 4. The levels were identified by inspection of the wave function expansion coefficients. Narrow crossings have not been drawn. The ν_1 energies depend on the *ad hoc* Morse potential and are uninteresting. The ν_2 and ν_3 energies for both HCCN and DCCN are closest to experiment if a linear structure with no barrier is assumed, but the variation is small for a wide range of perturbation p. The ν_4 energies, in particular for HCCN, are much too high in the linear case, and are in best agreement with experiment if a modest barrier is assumed. However, the ν_4 energies from these calculations are not reliable, since they are quite strongly affected by the freezing of the CCN bending

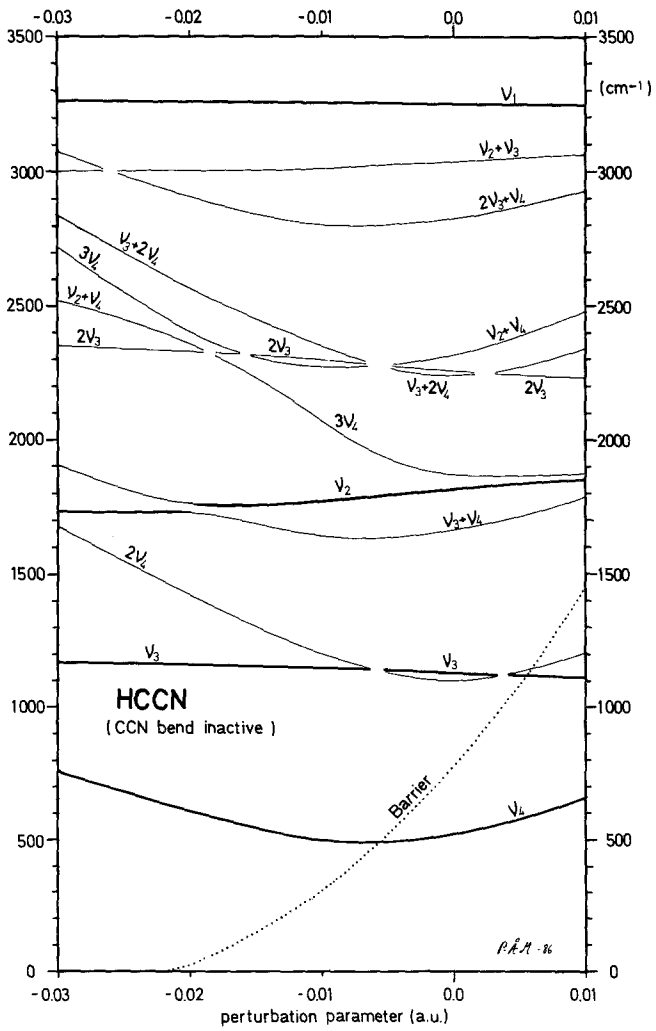

Fig. 3. Survey of HCCN vibration levels in the ν_4 to ν_1 energy region

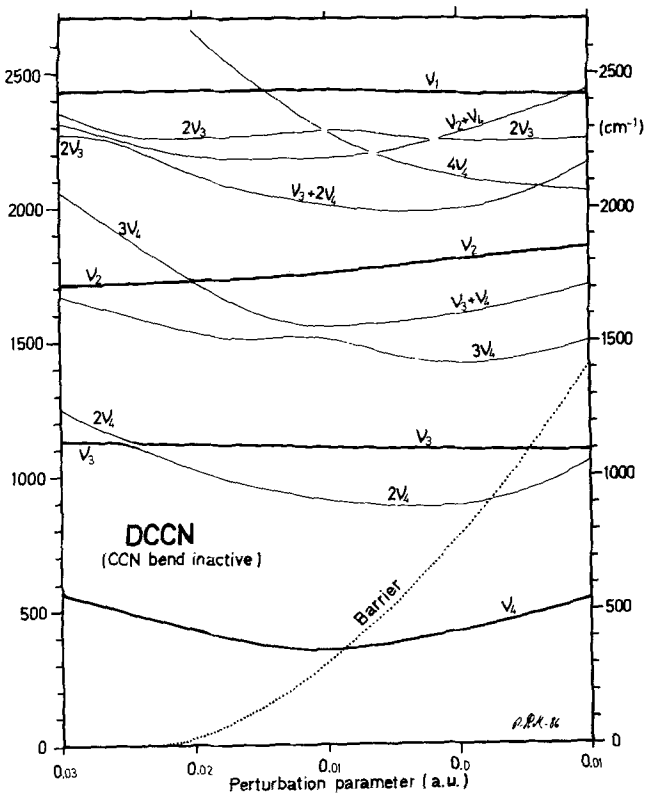

Fig. 4. Survey of DCCN vibration levels in the v_4 to v_1 energy region

modes. In this respect, they may be compared with the semi-rigid bender approximation, but they include dynamic interaction between ν_4 and the CC and CN stretching modes, and they also include the structure dependence of the "stiff" zero-point energies.

For the more limited energy range up to and including the ν_4 excitation energy, the CCN bending modes were released, and some calculations with $J \neq 0$ were included. The results are shown in Figs. 5 and 6. The first of these is drawn in a similar way to Figs. 3 and 4. It is now clear that the calculated ν_4 energy is always too high, also for the DCCN case. Again, they are closest to experiment if a small barrier is assumed, and become much too high in the linear and the strongly bent cases. The total variation of the ν_4 frequencies in the range of p values is larger than for the ν_2 and ν_3 frequencies, but since the "best" values are minimum points above the experimental values, there is still a considerable range of barrier heights which may be reasonable. The ν_5 and ν_6 frequencies depend directly on an assumed force constant and may not be compared with experiment.

Some results are summarized in Table 4, together with experimental values. The best agreement is found with barrier heights in the interval 28 to 776 cm^{-1}.

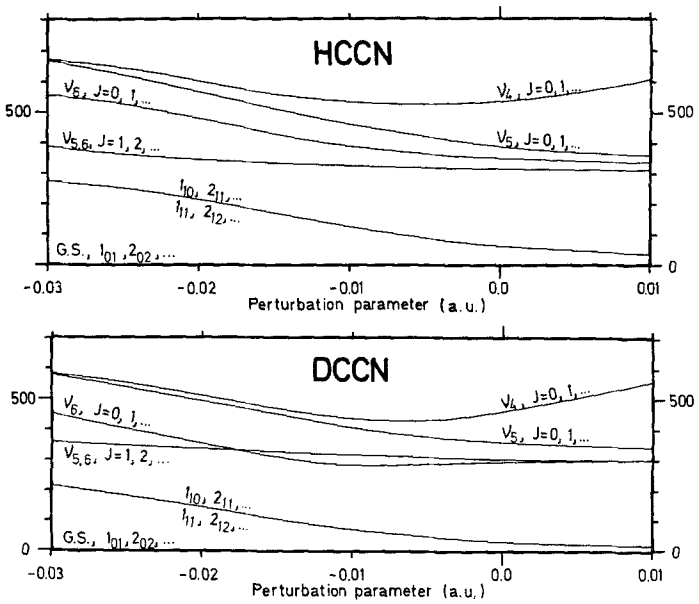

Fig. 5. HCCN and DCCN vibration and rotation levels up to v_4

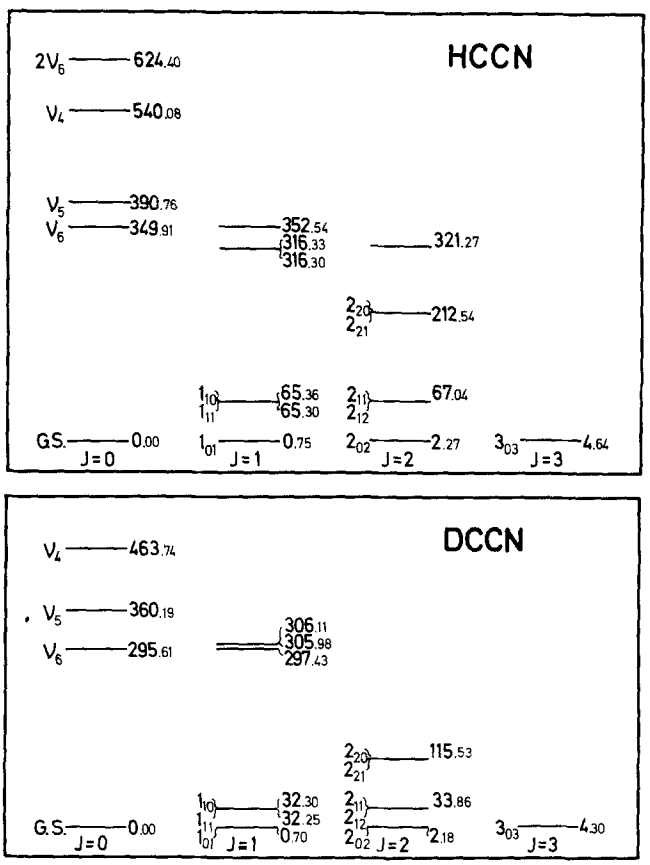

Fig. 6. HCCN and DCCN vibration and rotation levels up to v_4, calculated for the CCI+Dav potential function

Table 4. Excitation energies from variational calculation, as function of perturbation parameter p

p (a.u.)		−0.03	−0.02	−0.01	0.00	0.01	Exp[a]
Barrier (cm^{-1})		—	28	308	776	1450	?
(kcal/mol)		—	0.08	0.9	2.2	4.1	?
ν_1 (cm^{-1})[b,c]	HCCN	3258.6	3257.7	3255.1	3250.0	3245.2	3229.0
	DCCN	2439.8	2437.8	2432.7	2425.1	2420.8	2424.0
ν_2 (cm^{-1})[b]	HCCN	1730.8	1730.9	1769.4	1813.8	1851.0	1735.0
	DCCN	1715.9	1733.1	1757.1	1808.7	1854.9	1729.5
ν_3 (cm^{-1})[b]	HCCN	1167.8	1160.3	1146.5	1129.7	1113.9	1178.5
	DCCN	1128.6	1122.7	1108.1	1093.3	1092.8	1127.0
ν_4 (cm^{-1})	HCCN	671.7	607.6	554.0	540.1	610.4	458
	DCCN	588.3	—	441.5	463.7	561.3	405
ν_5 (cm^{-1})[c]	HCCN	670.5	567.6	462.3	390.8	362.1	369.5?
	DCCN	586.5	516.0	406.3	360.2	345.9	317.5?
ν_6 (cm^{-1})[c]	HCCN	556.7	482.8	391.5	349.9	336.2	369.5?
	DCCN	451.9	353.6	282.5	295.6	303.1	317.5?
$E_{K=1} - E_{K=0}$	HCCN	275.2	216.7	128.7	64.6	39.5	?
(cm^{-1})	DCCN	214.7	146.9	71.3	32.3	21.1	?

[a] Experimental values from [3]
[b] Calculated with ν_5, ν_6 frozen
[c] This value depends directly on an assumed force constant

In Fig. 5, some rotationally excited states have also been included. As indicated, each curve actually shows a number of closely spaced eigenstates, which cannot be resolved on this scale. However, some rotation excitations correlate with the CCH and CCN bending modes in the linear case, and are seen to have very high energies, which rapidly decrease with increasing barrier height for the bent molecules. These are the states responsible for the expected microwave satellites. In a qualitative sense, the rotation energies for the bent structure is in accordance with an extremely prolate rigid rotor, as can be seen in Fig. 6 (which was drawn for the non-perturbed case, with a barrier height of 776 cm^{-1}). However, even for the highest barriers, the $\Delta K = +1$ rotation excitation energies are quite far from that of a *rigid* rotor with the *equilibrium* moments of inertia. This is mainly due to the non-negligible wave function amplitude for nearly linear structures, but for the low barriers there is also some centrifugal distortion. Therefore, calculation of equilibrium structure from observed rotation excitation energies alone cannot be done without a fairly detailed knowledge of the wave function. The $\Delta K = 0$ transitions, giving the B rotation constant, are in better accordance with a rigid rotor model based on equilibrium structure, but since our variational transition energies are differences between separately optimized energies, each of which contain large terms, the accuracy of the variational values is not sufficient to give a good B constant. For that purpose, the semi-rigid bender calculation (see Table 3) gives more reliable values. As an example, the unperturbed CCI+Dav potential gives $B = 10703$ MHz in the semi-rigid bender calculation, or a 1_{01} excitation energy of 0.71 cm^{-1}, as compared to the variational energy difference of 0.75 cm^{-1}. Naturally, the semi-rigid bender results are also in close accordance with what is obtained from a rigid molecule with the CCI+Dav equilibrium

geometry. The experimental result $B = 10986$ MHz of Saito et al. [4] is in reasonable agreement with our results. The discrepancy is due to an error in our CC and CN bond lengths, which are slightly too large. However, their statement that the B value demands the sum of the CC and CN bond lengths to be within the narrow range of 2.48–2.50 Å, seems to be in error. As a specific counterexample, consider a rigid molecule with equilibrium structure obtained by Rice et al. [8] with the TZP basis. This gives a B value of 11029 MHz, above the experimental value, and yet with a bond length sum in excess of 2.53 Å. If anything, the experiment thus suggests that their bond lengths are slightly too small. The limit quoted by Saito et al. is obtained only by making the assumption that the molecule is linear.

For all calculated states, expectation values of some quantities of interest were also calculated. Some of these are tabulated, for the ground state only, in Table 5. Also, the variation of the expectation value of the cosine of the CCH angle and the CC and CN bond lengths with the perturbation parameter p is shown, for the DCCN case, in Fig. 7. The following features are clearly seen: If the equilibrium structure is linear, the average CCH bending angle is still considerable. As a consequence, since this bending is coupled to the variations of the CC and CN bond lengths, the latter deviate unusually much from the equilibrium quantities in the barrier-free region. Also, these deviations show the expected isotopic variation from HCCN to DCCN. For low barriers, the deviation and therefore also the isotopic variation is small. Finally, for large barriers, there is

Table 5. Selected expectation values and isotopic variation, related to perturbation parameter p and hence to barrier height

p (a.u.)		−0.03	−0.02	−0.01	0.00	0.01
Barrier (cm^{-1})		—	28	308	776	1450
mean θ_{CCH}[a]	equil.	180.0	158.34	145.65	138.33	132.44
(deg.)	HCCN	160.91	157.36	150.92	142.15	134.76
	DCCN	162.63	158.69	150.72	141.26	134.25
	HCCN-DCCN	−1.72	−1.33	0.20	0.89	0.51
mean R_{CC}[b]	equil.	1.3165	1.3337	1.3528	1.3634	1.3712
(Å)	HCCN	1.3363	1.3405	1.3490	1.3619	1.3729
	DCCN	1.3344	1.3389	1.3495	1.3637	1.3739
	HCCN-DCCN	0.0019	0.0016	−0.0005	−0.0018	−0.0010
mean R_{CN}[b]	equil.	1.2247	1.2163	1.2086	1.2050	1.2026
(Å)	HCCN	1.2250	1.2232	1.2197	1.2148	1.2110
	DCCN	1.2258	1.2239	1.2195	1.2141	1.2107
	HCCN-DCCN	0.0008	−0.0007	0.0002	0.0007	0.0003
Zero-point vibration						
energies	HCCN	3711	3594	3658	3764	3839
(cm^{-1})	DCCN	3188	3092	3167	3255	3313
	HCCN-DCCN	523	502	491	509	526

[a] Mean is defined as arccos (expectation value of cosine)
[b] Mean is defined as expectation value

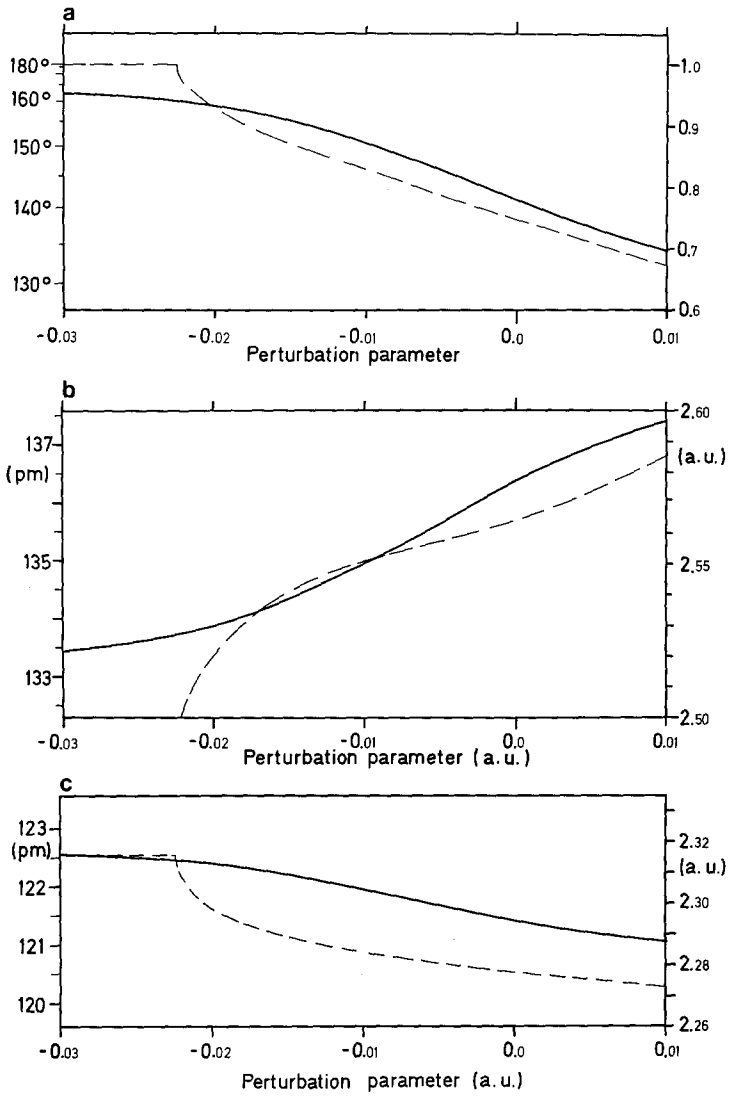

Fig. 7. Expectation values of structural parameters for DCCN

a deviation in the other direction due to large anharmonicity of the CCH bending, and again there is the expected isotopic dependence. Superimposed on these deviations there is also the ever-present lengthening of the CC and CN bonds due to their own anharmonicity.

The method outlined here has the following merits. It gives accurate results for a well-defined range of model potentials with no approximations in the kinetic Hamiltonian. In contrast to methods based on a simplified kinetic Hamiltonian, all errors come from the potential. The accuracy of the simpler methods can be assessed by comparison with the full variational results. Furthermore, if a reason-

ably good potential is assumed to be included in the range we have investigated, the results not only pinpoint the need to observe transitions involving the very sensitive rotations around the CCN axis, but also provide an interpretation of such future data in terms of barrier height. Finally, since the existing program calculates a full vibration-rotation wave function, it is capable of providing expectation and transition values of any operators defined on that space. Full technical details of the vibration-rotation calculations will be published elsewhere [20].

The variational calculations were technically successful, but those calculated quantities which can be compared to existing experimental data are too insensitive to the barrier height to allow a more precise estimate of the barrier height. However, based on ν_4 energies, the barrier height is estimated to lie in the range 1 ± 0.5 kcal/mol.

Acknowledgement. We are grateful to Julia E. Rice and Henry F. Schaefer for sending us the manuscript of their article [8] prior to publication. This research was supported by a grant from the Swedish Natural Science Research Council.

References and notes

1. Bernheim RA, Kempf RJ, Humber PW, Skell PS (1964) J Chem Phys 41:1156
   Bernheim RA, Kempf RJ, Gramas JV, Skell PS (1965) J Chem Phys 43:196
   Bernheim RA, Kempf RJ, Reichenbecher EF (1970) J Magn Reson 3:5
2. Wasserman E, Yager WA, Kuck VJ (1970) Chem Phys Lett 7:409
3. Dendramis A, Leroi G E (1977) J Chem Phys 66:4334
4. Saito S, Endo Y, Hirata E (1984) J Chem Phys 80:1427
5. Harrison JF, Dendramis A, Leroi GE (1978) J Am Chem Soc 100:4352
6. Zandler ME, Goddard JD, Schaefer III HF (1979) J Am Chem Soc 101:1072
7. Kim KS, Schaefer III HF, Radom L, Pople JA, Binkley JS (1983) J Am Chem Soc 105:4148
8. Rice JE, Schaefer III HF: J Chem Phys, to be published
9. Karlström G, private communications
10. Roos BO, Taylor PR, Siegbahn PEM (1980) Chem Phys 48:157; Roos BO (1980) Int J Quantum Chem Symp 14:175; Siegbahn PEM, Almlöf J, Heiberg A, Roos BO (1981) J Chem Phys 74:2384
11. Siegbahn PEM (1981). In: Carbó R (ed) Current Aspects of Quantum Chemistry: Proceedings of the International Congress, Barcelona, Spain, 1981. Elsevier, Amsterdam
12. Davidson ER (1974). In: Daudel R, Pullman B (eds) The world of quantum chemistry. Riedel, Amsterdam
13. Huzinaga S (1965) J Chem Phys 42:1293
14. Dunning Jr TH (1970) J Chem Phys 53:2823
15. Almlöf J (1974) MOLECULE Integral Program Description, University of Stockholm, Sweden, Institute of Theoretical Physics, Report 74–29
16. Saebö (1979) MOLFORC Program Description, Technical Report, University of Oslo, Norway
17. Taylor PR (1984) J Comput Chem 5:589
18. Bunker PR, Landsberg BM (1977) J Mol Spectrosc 67:374;
    Bunker PR, Landsberg BM, Windewisser BP (1978) J Mol Spectrosc 74:9
19. Hougen JT, Bunker PR, Johns JWC (1970) J Mol Spectrosc 34:136
20. Malmquist PÅ: to be published